ADVANCES IN ATMOSPHERIC SCIENCES, VOL. 31, MARCH 2014, 344–354

Interference of the East Asian Winter Monsoon in the Impact of ENSO on the East Asian Summer Monsoon in Decaying Phases

FENG Juan* and CHEN Wen

Center for Monsoon System Research, Institute of Atmospheric Physics, Chinese Academy of Sciences, Beijing 100029

(Received 6 June 2013; revised 22 July 2013; accepted 29 July 2013)

ABSTRACT

The variability of the East Asian winter monsoon (EAWM) can be divided into an ENSO-related part ($EAWM_{EN}$) and an ENSO-unrelated part ($EAWM_{res}$). The influence of $EAWM_{res}$ on the ENSO–East Asian summer monsoon (EASM) relationship in the decaying stages of ENSO is investigated in the present study. To achieve this, ENSO is divided into four groups based on the $EAWM_{res}$: (1) weak $EAWM_{res}$–El Niño ($WEAWM_{res}$–EN); (2) strong $EAWM_{res}$–El Niño ($SEAWM_{res}$–EN); (3) weak $EAWM_{res}$–La Niña ($WEAWM_{res}$–LN); (4) strong $EAWM_{res}$–La Niña ($SEAWM_{res}$–LN). Composite results demonstrate that the $EAWM_{res}$ may enhance the atmospheric responses over East Asia to ENSO for $WEAWM_{res}$–EN and $SEAWM_{res}$–LN. The corresponding low-level anticyclonic (cyclonic) anomalies over the western North Pacific (WNP) associated with El Niño (La Niña) tend to be strong. Importantly, this feature may persist into the following summer, causing abundant rainfall in northern China for $WEAWM_{res}$–EN cases and in southwestern China for $SEAWM_{res}$–LN cases. In contrast, for the $SEAWM_{res}$–EN and $WEAWM_{res}$–LN groups, the $EAWM_{res}$ tends to weaken the atmospheric circulation anomalies associated with El Niño or La Niña. In these cases, the anomalous WNP anticyclone or cyclone tend to be reduced and confined to lower latitudes, which results in deficient summer rainfall in northern China for $SEAWM_{res}$–EN and in southwestern China for $WEAWM_{res}$–LN. Further study suggests that anomalous $EAWM_{res}$ may have an effect on the extra-tropical sea surface temperature anomaly, which persists into the ensuing summer and may interfere with the influences of ENSO.

Key words: East Asian winter monsoon, ENSO, East Asian summer monsoon

Citation: Feng, J., and W. Chen, 2014: Interference of the East Asian winter monsoon in the impact of ENSO on the East Asian summer monsoon in decaying phases. *Adv. Atmos. Sci.*, **31**(2), 344–354, doi: 10.1007/s00376-013-3118-8.

1. Introduction

The East Asian summer monsoon (EASM) is an important subsystem of the Asian summer monsoon (Tao and Chen, 1987; Ding, 1992; Chang et al., 2000a, 2000b; Huang et al., 2003). The year-to-year variability of the EASM tends to cause severe droughts and floods in East Asian regions, resulting in human casualties and economic losses (Huang et al., 2003). The El Niño-Southern Oscillation (ENSO) is widely considered as the most important external forcing acting upon the variation of the EASM (Zhang et al., 1999; Wu and Wang, 2002; Huang et al., 2004; Chan and Zhou, 2005; Zhou et al., 2006; Zhou and Chan, 2007), and their relationship exhibits distinct features during the different stages of ENSO. During a developing El Niño summer, negative rainfall anomalies appear in northern China, while during a decaying El Niño summer, rainfall anomalies show a different distribution, with negative anomalies in northern and southern China, and positive anomalies over the Yangtze River Valley (Huang and Wu, 1989; Liu and Ding, 1992; Chen, 2002; Wu et al., 2003). For example, the extremely severe floods in the Yangtze River Valley in 1998 happened during the decaying summer of the extraordinarily strong 1997/98 El Niño (Lau and Weng, 2001).

Despite knowledge of the relationship, prediction of the EASM based on ENSO is not always accurate. One reason may be that there are many factors impacting the EASM, such as soil moisture, ice cover and regional SST anomalies (e.g., Lau, 1992; Huang et al., 2003; Wu and Kirtman, 2007; Ding et al., 2010; Zhang et al., 2011; Wu et al., 2012a), while another important reason may be the instability of the ENSO–EASM relationship (Wang, 2002). This instability may be caused by changes in ENSO behavior. For example, El Niño exerts different impacts on the following EASM when the onset time of El Niño occurs during different seasons (Li and Shou, 2000). Xue and Liu (2008) suggested that a strong ENSO tends to have a robust impact on the EASM, while a moderate ENSO has a weak impact. The El Niño–EASM relationship also depends on the location of warm SST anomalies (Lin and Yu, 1993; Weng et al., 2007; Feng et al., 2011). When these are located in the tropical eastern Pacific (EP)—named EP-type El Niño, or conventional El Niño–the EASM is characterized by positive rainfall anoma-

* Corresponding author: FENG Juan
Email: juanfeng@mail.iap.ac.cn

lies over the Yangtze River Valley during the decaying summer of El Niño. In contrast, when the warm SST anomalies appear in the tropical central Pacific (CP)—named CP-type El Niño, or El Niño Modoki—the positive rainfall belt moves northward to the Huaihe–Yellow River, and the Yangtze River region experiences negative rainfall anomalies (Feng et al., 2011).

Meanwhile, some recent studies have pointed out that the instability of the ENSO–EASM relationship could be caused by extra-tropical influences (Chan and Zhou, 2005; Rong et al., 2010; Yoon and Yeh, 2010; Wu et al., 2012b). Yoon and Yeh (2010) reported that the Pacific Decadal Oscillation (PDO) disrupts the linkage between El Niño and the following Northeast Asian summer monsoon (NEASM) through inducing the Eurasian pattern in the mid-high latitudes. Wu et al. (2012b) suggested that the spring North Atlantic Oscillation (NAO) could strengthen the ENSO–EASM relationship. The spring NAO tends to trigger a tripole SST anomaly in the North Atlantic region, which can persist into the following summer and induce a Rossby wave in the mid-high latitudes and a Gill–Matsuno wave over the low latitudes. These two waves enhance the ENSO–EASM relationship.

The East Asian winter monsoon (EAWM) is another important climate system, which is characterized by strong northeasterlies along the eastern edge of the Siberian High and the coast of East Asia (e.g., Ding, 1994; Chen et al., 2005; Wang and Chen, 2010). During the EAWM season, ENSO generally reaches its mature phase and has the most prominent impact on the climate. Hence, a warm ENSO tends to lead to a weak EAWM through inducing southwesterly winds over the coast of East Asia, while a cool ENSO causes a reversed EAWM condition (Zhang et al., 1996; Chen, 2002). The vast majority of studies have concentrated on the impacts of ENSO on the EAWM (Tomita and Yasunari, 1996; Zhang et al., 1996; Chen et al., 2000; Chen, 2002; Wang et al., 2008; Zhou and Wu, 2010). However, the effect of modulation of the EAWM on the impact of ENSO has rarely been examined. Chen et al. (2013) divided the EAWM into two components: an ENSO-related part—named $EAWM_{EN}$, arising from the tropical process—and an ENSO-unrelated part, named $EAWM_{res}$, arising from the extra-tropical process. They found that the $EAWM_{EN}$ explains only 35% of the total EAWM variation, while the variation explained by $EAWM_{res}$ reaches up to 65%, demonstrating that the $EAWM_{res}$ accounts for most of the EAWM variation. Thus, we wonder whether $EAWM_{res}$ has a modulation effect on the ENSO–EASM relationship; and hence, in the present study, the impact of $EAWM_{res}$ on the ENSO–EASM relationship during the decaying phase of ENSO is investigated—the aim being to aid our understanding of the reasons behind the instability of the ENSO–EASM relationship.

The structure of the paper is as follows. The data and methods employed are introduced in section 2. Section 3 reveals the modulation effect of the $EAWM_{res}$ on the impact of ENSO on summer rainfall anomalies in China. The corresponding atmospheric circulation anomalies responsible for the rainfall anomalies are then analyzed in section 4. Section 5 discusses the possible mechanisms through which the $EAWM_{res}$ modulates the ENSO–EASM relationship; and finally, section 6 summarizes the key findings of the study.

2. Data and methods

Monthly mean ERA-40 reanalysis data, including winds and geopotential heights, derived from the European Centre of Medium-Range Weather Forecasts (ECMWF), are used in the present study (Uppala et al., 2005). The dataset covers the period from September 1957 to August 2002, and has a horizontal resolution of $2.5^\circ \times 2.5^\circ$ and a 17-level vertical resolution from 1000 hPa to 1 hPa. Also used are rainfall data from 160 stations across China, obtained from the Chinese Meteorological Data Center. This dataset is available from 1951 to the present day. In addition, Hadley Center Global Sea Ice and Sea Surface Temperature (HadISST) monthly SST data are employed, spanning the period from 1870 to the present day, with a horizontal resolution of $1^\circ \times 1^\circ$ (Rayner et al., 2003). For consistency, the data period from September 1957 to August 2002 is considered in this study. The interdecadal variation with a period over seven years has been removed from the original data using the Lancos filter in order to highlight the interannual variation (Duchon, 1979).

The interannual variability of the EAWM is estimated by the index (EAWMI) proposed by Yang et al. (2002), which is defined by the meridional 850-hPa winds averaged over the region (20°–40°N, 100°–140°E). To investigate the roles of the $EAWM_{res}$ in the impact of ENSO on the following EASM, the ENSO-related EAWMI is removed from the EAWM through the linear regression method (Chen et al., 2013) (Fig. 1). The obtained EAWM part is denoted as $EAWM_{res}$ and the index as $EAWMI_{res}$. A positive (negative) $EAWMI_{res}$ indicates a weak (strong) EAWM, and strong (weak) EAWM winters are selected according to $EAWMI_{res} > 0$ (< 0). ENSO events are identified by the normalized winter mean (Dec–Jan–Feb) Niño3 (5°S–5°N, 150°–90°W) index being greater than 0.5, and the maximum SST anomaly in the central-eastern Pacific exceeding 1°. The ENSO events are then further sorted into four groups: (1) weak $EAWM_{res}$ with El Niño ($WEAWM_{res}$–EN); (2) strong $EAWM_{res}$ with El Niño ($SEAWM_{res}$–EN); (3) weak $EAWM_{res}$ with La Niña ($WEAWM_{res}$–LN); (4) strong

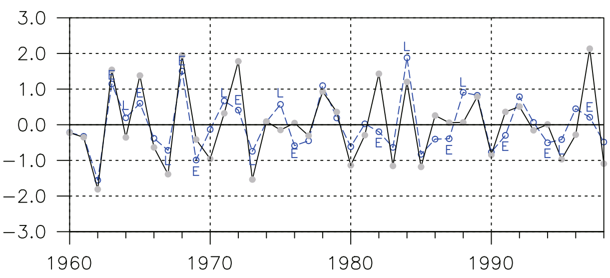

Fig. 1. Time series of the normalized EAWMI (solid line) and the ENSO-unrelated EAWMI (dashed line). "E" and "L" denote El Niño and La Niña years, respectively.

Table 1. Distribution of the ENSO events based on the $EAWMI_{res}$.

	El Niño	La Niña
Weak $EAWMI_{res}$	1963, 1965, 1968, 1972, 1997	1964, 1971, 1975, 1984, 1988
Strong $EAWMI_{res}$	1969, 1976, 1982, 1987, 1991, 1994	1967, 1973, 1995

$EAWM_{res}$ with La Niña ($SEAWM_{res}$–LN). The cases for the four groups are shown in Table 1.

3. Modulation effect of $EAWM_{res}$ on the impact of ENSO on summer rainfall in China

The general lagged influence of ENSO on summer rainfall in China is depicted in Fig. 2, which shows the composite rainfall anomalies during the decaying summer of the El Niño and La Niña cases. The rainfall anomalies in eastern China present alternative positive and negative values in the north–south direction for both the El Niño and La Niña events. During El Niño decaying summers, above-normal rainfall is located in northern China and over the Yangtze River valley, while below-normal rainfall is seen over the Huaihe River valley (Fig. 2a). In contrast, the rainfall anomaly distribution shows an opposite feature during decaying summers of La Niña, with wet conditions over the Huaihe River valley and dry conditions in northern China and over the Yangtze River valley (Fig. 2b). These rainfall anomaly distributions are consistent with previous results (Huang and Wu, 1989; Chen, 2002).

The ENSO–EASM relationship is re-investigated in Fig. 3 based on the classification of ENSO into the four different $EAWM_{res}$ groups, in which the rainfall anomalies in the following summer for $WEAWM_{res}$–EN, $SEAWM_{res}$–EN, $WEAWM_{res}$–LN and $SEAWM_{res}$–LN are shown. Under El Niño conditions, the rainfall anomalies in China display different spatial patterns between the weak $EAWM_{res}$ and strong $EAWM_{res}$ (Figs. 3a and b), with the most pronounced difference occurring in northern China (Fig. 3e). When the $EAWM_{res}$ is in a weak state, northern China experiences significantly positive rainfall anomalies (Fig. 3a). Conversely, when the $EAWM_{res}$ is in a strong state, northern China is covered by negative rainfall anomalies (Fig. 3b). For the decaying summer of the two groups of La Niña cases, the significant difference in summer rainfall anomalies is dominantly seen in southwestern China (Fig. 3f). Severe droughts happen there in the $WEAWM_{res}$–LN cases (Fig. 3c), whereas floods occur in the $SEAWM_{res}$–LN cases (Fig. 3d). Comparing Fig. 2 to Fig. 3, one can see that the ENSO–EASM relationship changes under $EAWM_{res}$ conditions. Hence, the $EAWM_{res}$ may play an active role in the influence of ENSO on the following EASM.

4. Anomalous atmospheric circulations responsible for the abnormal rainfall in China

The low-level anomalous anticyclone (cyclone) over the western North Pacific (WNP) is the main anomalous atmospheric circulation that links ENSO to the following summer's rainfall in East Asia (Zhang et al., 1999; Wang et al., 2000). Figures 4 and 5 present the composite evolutions of the 850-hPa wind anomalies for the $WEAWM_{res}$–EN, $SEAWM_{res}$–EN, $WEAWM_{res}$–LN and $SEAWM_{res}$–LN cases, respectively. The results show that the anomalous WNP anticyclone is very strong and significant during $WEAWM_{res}$–EN winters (Fig. 4a), but very weak and insignificant for $SEAWM_{res}$–EN winters (Fig. 4b). This difference can be attributed to the different circulation anomalies induced by the $EAWM_{res}$. A weak $EAWM_{res}$ winter is characterized by anomalous anticyclonic flow over the WNP (Chen et al., 2013, Fig. 5), and a strong $EAWM_{res}$ winter has the reverse features. Consequently, when an El Niño is combined with a weak $EAWM_{res}$, the anomalous WNP anti-

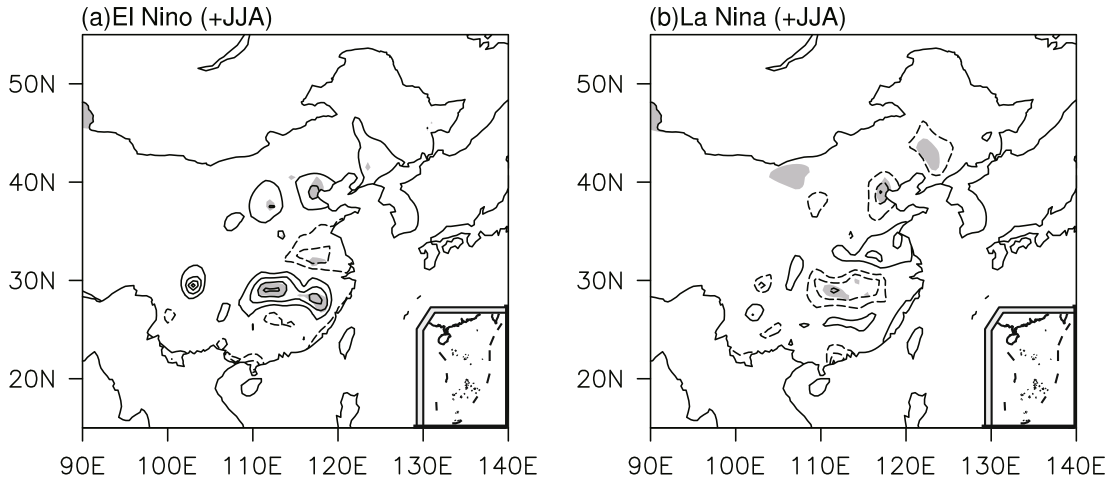

Fig. 2. Composite summer mean (JJA) rainfall anomalies during the decaying phases of the (a) El Niño and (b) La Niña events. The shading indicate the 90% confidence level according to a two-tailed Student's t-test.

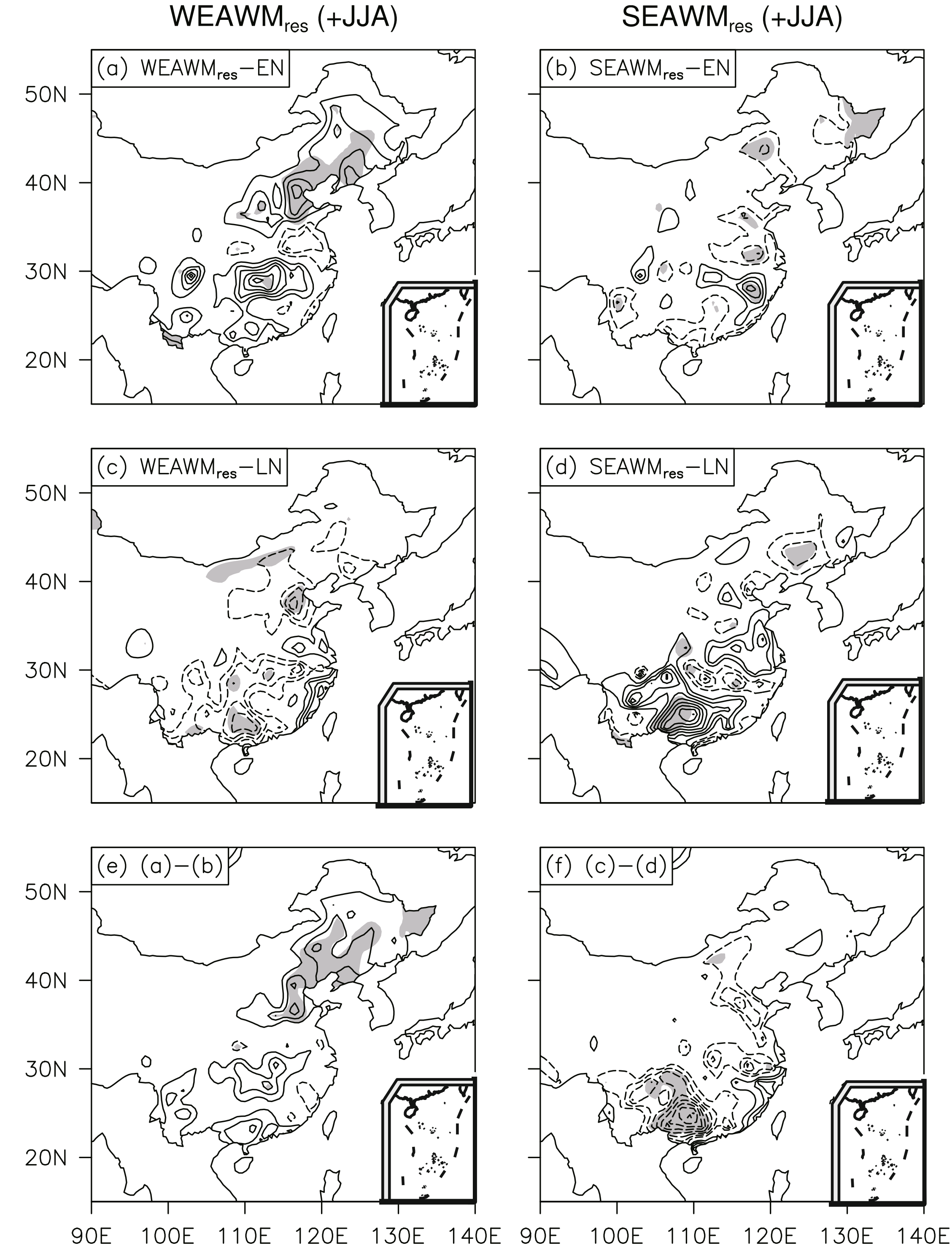

Fig. 3. Composite summer mean (+JJA) rainfall anomalies during the (a) weak EAWM$_{res}$–El Niño; (b) strong EAWM$_{res}$–El Niño; (c) weak EAWM$_{res}$–La Niña; and (d) strong EAWM$_{res}$–La Niña. (e) The difference between (a) and (b). (f) The difference between (c) and (d). The contour interval is 10 mm month^{-1} for (a)–(d), while it is 15 mm mon^{-1} for (e) and (f). The shading indicate the 90% confidence level according to a two-tailed Student's *t*-test.

cyclone associated with El Niño tends to be strengthened and covers a larger domain due to the negative vorticity arising from a weak EAWM$_{res}$. In contrast, when an El Niño occurs together with a strong EAWM$_{res}$, the anomalous WNP anticyclone tends to be substantially weakened. For the La Niña cases, similar mechanisms can be detected in Figs. 5a and d. Thus, the anomalous WNP anticyclone (cyclone) associated with ENSO may be enhanced (weakened) in winter by

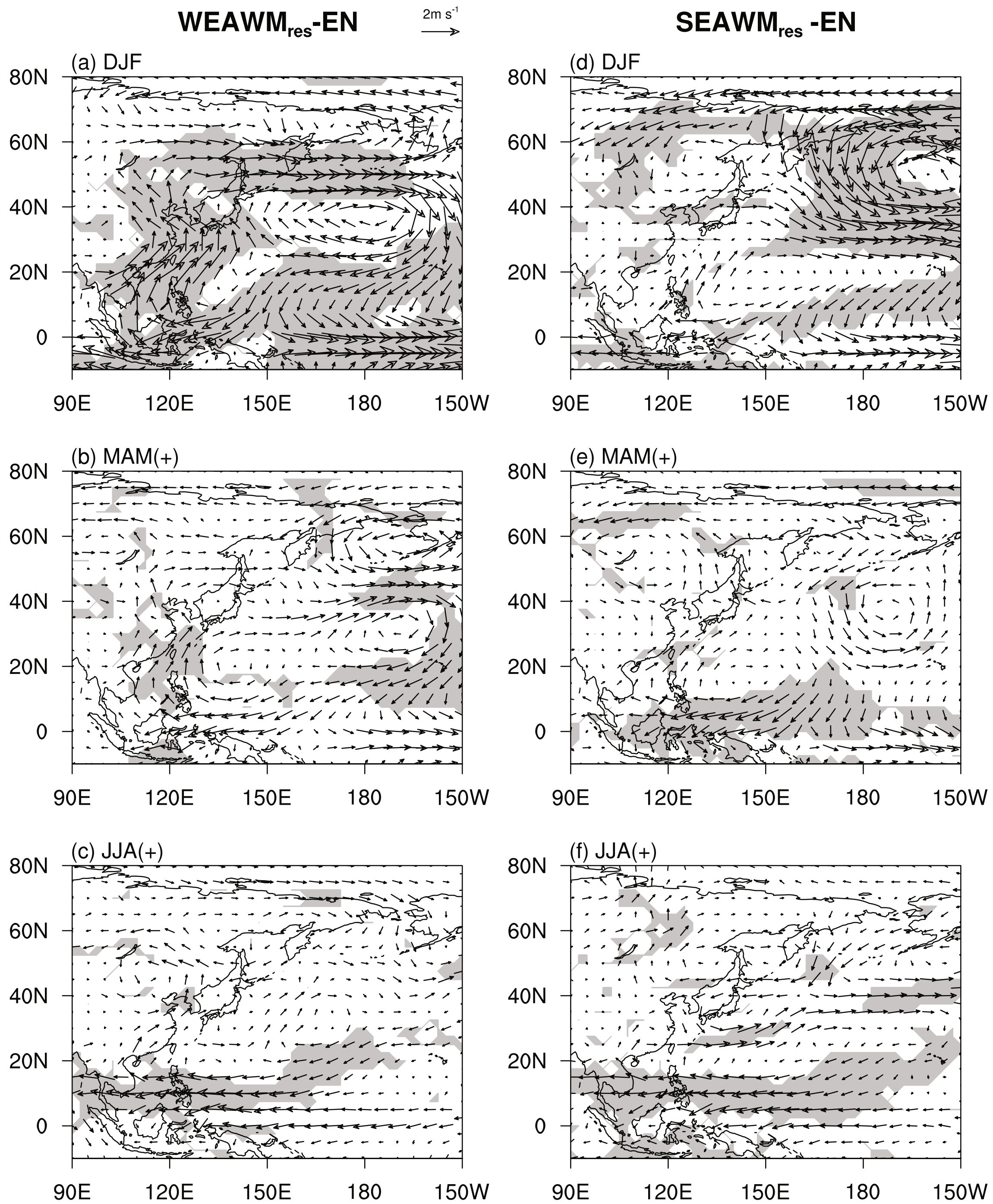

Fig. 4. Composite 850-hPa wind anomalies in the (a, d) DJF; (b, e) MAM (+); and (c, f) JJA (+). The left (right) column is for the WEAWM$_{res}$–EN (SEAWM$_{res}$–EN) groups. The shading indicates the 90% confidence level according to a two-tailed Student's t-test.

an anomalous EAWM$_{res}$. This effect of the EAWM$_{res}$ on the atmospheric responses to ENSO may further influence the atmospheric circulations in the following spring and summer.

During the ensuing spring and summer of WEAWM$_{res}$–EN events, the wintertime enhanced WNP anticyclonic anomalies still cover a large domain and extend to the high latitudes (Figs. 4b and c), which favors the transportation of more water vapor from the South China Sea to northern China and in turn leads to more substantial rainfall there (Fig. 3a). However, for SEAWM$_{res}$–EN events, the wintertime suppressed WNP anticyclone is located in the low latitudes during the following spring and summer (Figs. 4d–f), thereby confining the water vapor to the low latitudes and then causing less summer rainfall in northern China (Fig. 3b).

Under La Niña conditions, the evolution of the WNP cyclone has a similar feature to that under El Niño conditions.

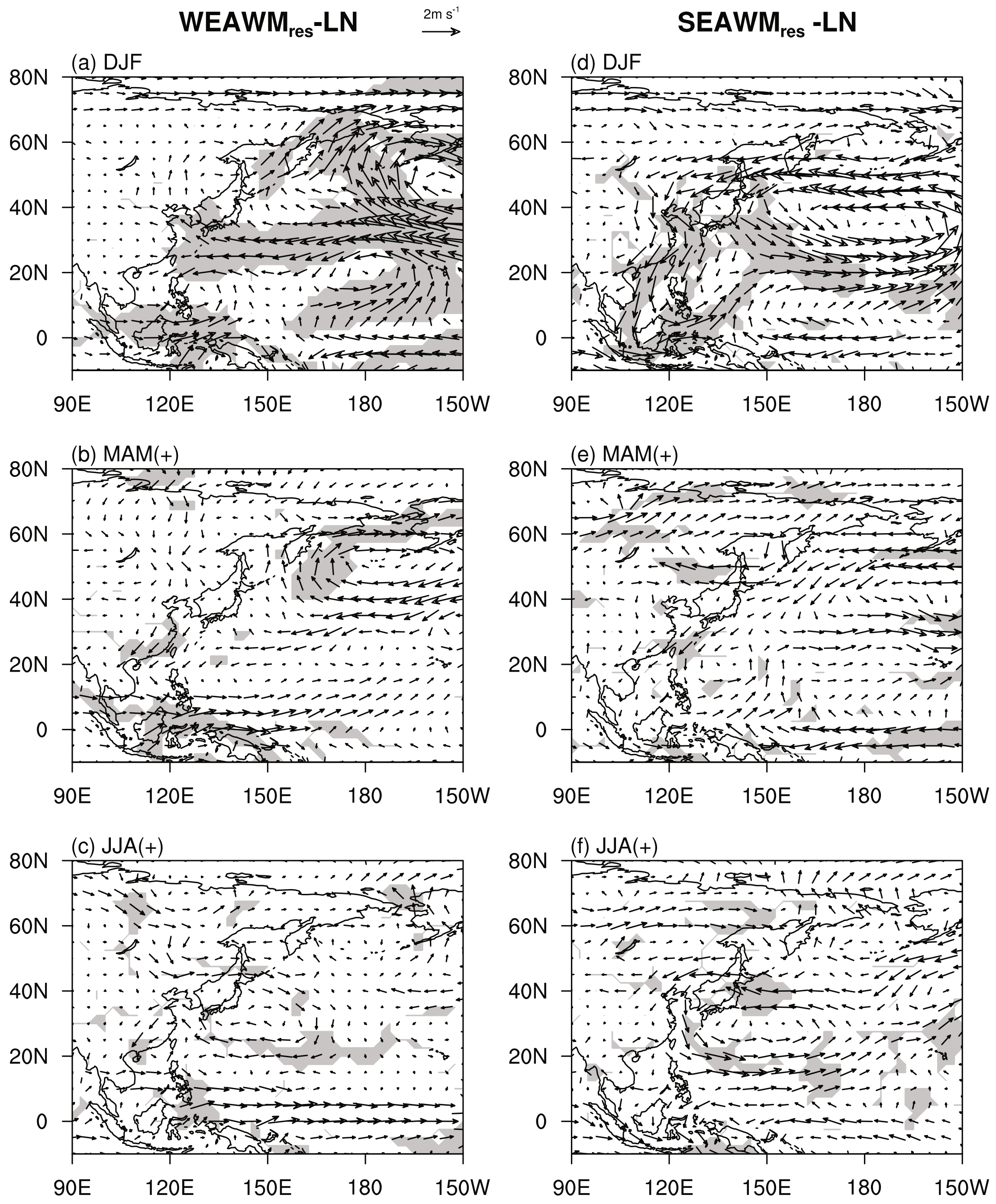

Fig. 5. The same as Fig. 4, but for the WEAWM$_{res}$–LN and SEAWM$_{res}$–LN cases.

During the SEAWM$_{res}$–LN cases, the anomalous WNP cyclone strengthened by the strong EAWM$_{res}$ in the winter covers a larger region in East Asia during the subsequent summer (Fig. 5f). The anomalous northeasterly winds on the western side of this cyclone enhance the convergence in southwestern China. In addition, weak anomalous southwesterly winds are observed in southwestern China. Hence, more substantial rainfall is caused in southwestern China (Fig. 3d). However, during the WEAWM$_{res}$–LN cases (Figs. 5a–c), the weakened anomalous WNP cyclone in the winter is still suppressed and confined to lower latitudes in the following spring and summer, transporting the water vapor from the East China Sea to the South China Sea. In such cases, less rainfall is observed in southwestern China.

As is known, the meridional winds along the coast of East Asia are an important feature of the EASM. Figure 6 presents the temporal evolutions of composite meridional wind anomalies averaged from 110°E to 130°E for the four groups as indicated in Table 1. In winter, the anomalous WNP anticyclone induced by El Niño generates anomalous southerlies over East Asia. In the case of $WEAWM_{res}$–EN, the southerly anomalies are enhanced by the weak $EAWM_{res}$ and extend to middle and high latitudes from winter to the following summer (Fig. 6a). In contrast, in the case of $SEAWM_{res}$–EN, the southerly anomalies stretch only to the mid-latitudes and are then broken off by the northerly anomalies associated with strong $EAWM_{res}$ (Fig. 6b). Therefore, El Niño combined with weak $EAWM_{res}$ generally gives rise to stronger meridional winds and causes more rainfall in northern China. In the La Niña events, the anomalous northerly winds associated with La Niña are weakened in a weak $EAWM_{res}$ winter and enhanced in a strong $EAWM_{res}$ winter. Subsequently, the weak northerly anomalies are broken off in $WEAWM_{res}$–LN cases, but in $SEAWM_{res}$–LN cases the strong northerly anomalies are able to persist into the following summer (Figs. 6c and d).

Figure 7 presents the evolutions of the anomalous 500-hPa geopotential heights for the $WEAWM_{res}$–EN and $SEAWM_{res}$–EN groups. When El Niño occurs together with a weak $EAWM_{res}$, the anomalous wintertime atmospheric circulation exhibits a western Pacific (WP) teleconnection pattern over the North Pacific region, with the positive pole centered west of Japan and the negative pole centered over the Kamchatka Peninsula (Fig. 7a). When El Niño is combined with a strong $EAWM_{res}$, the anomalous atmospheric teleconnection in the winter exhibits a different pattern from that during the weak $EAWM_{res}$. The negative pole moves eastward to the North Pacific and the positive pole shifts to the north-

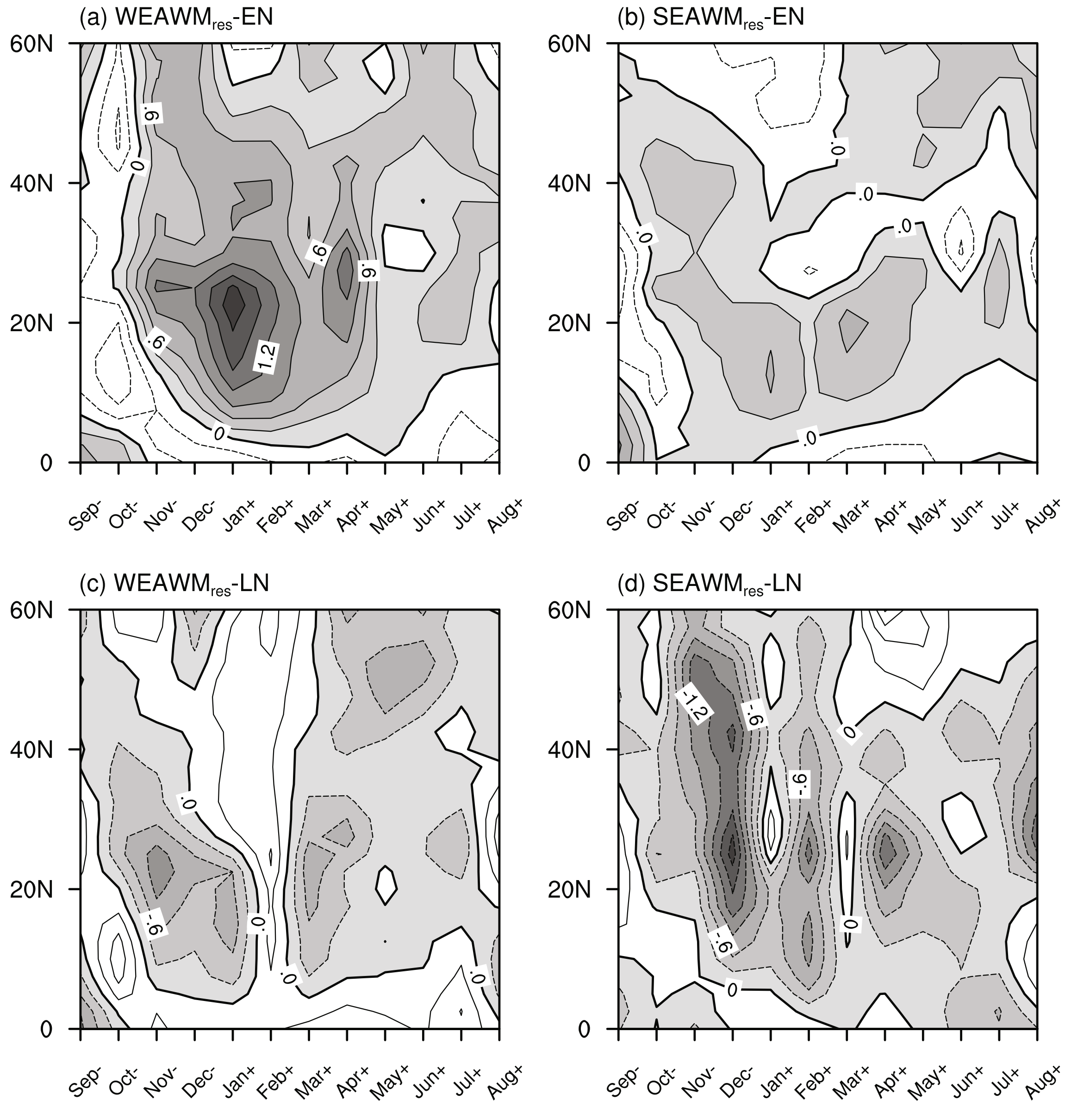

Fig. 6. Temporal evolutions of composite meridional wind anomalies averaged from 110° to 130°E during the (a) weak $EAWN_{res}$–El Niño; (b) strong $EAWN_{res}$–El Niño; (c) weak $EAWM_{res}$–La Niña; and (d) strong $EAWM_{res}$–La Niña. The contour interval is 0.3 m s^{-1}. Shading is applied for highlighting.

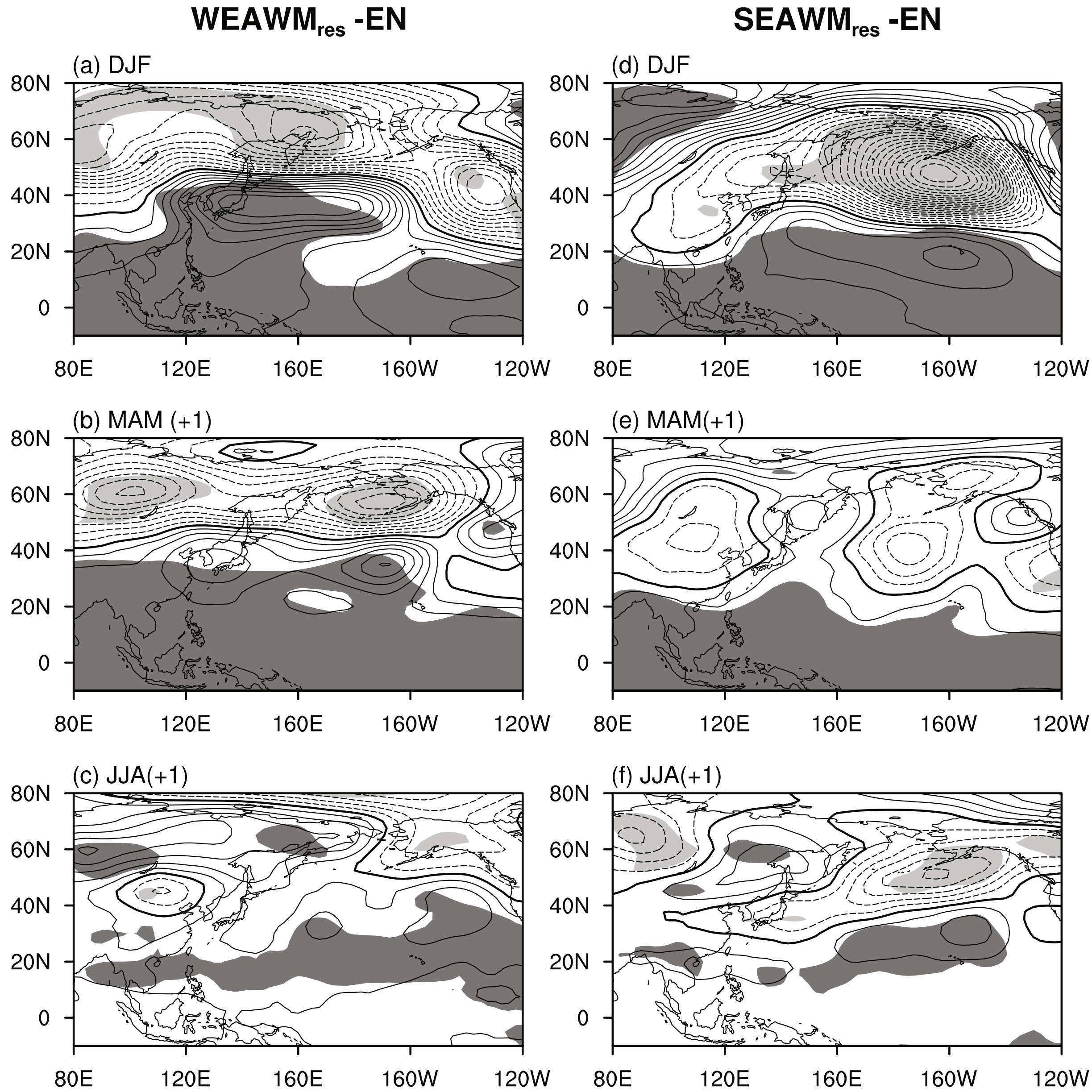

Fig. 7. The same as Fig. 4, but for the 500-hPa geopotential heights. The contour interval is 4 gpm. The solid (dashed) lines denote positive (negative) anomalies. The shading indicates the 90% confidence level, according to a two-tailed Student's t-test.

central Pacific (Fig. 7d). Hence, the Pacific North American (PNA) pattern is formed during the SEAWM$_{res}$–EN events (Fig. 7d). In such a case, the positive geopotential height anomaly around the East Asian region is suppressed more extremely compared to that during WEAWM$_{res}$–EN events (Fig. 7a), which is consistent with the results shown in Fig. 4. These different atmospheric responses in the winter impart very distinct signals to the subsequent seasons. The strong (weak) and large-scale (small-scale) positive geopotential height anomalies around the WNP persist to the following spring and summer for WEAWM$_{res}$–EN (SEAWM$_{res}$–EN) cases, consistent with the strong (weak) WNP anticyclone at the low level in Fig. 4.

Importantly, the 500-hPa geopotential height anomalies during decaying summers of El Niño are closely related to the anomalous western Pacific subtropical high (WPSH), which is another salient factor responsible for the abnormal East Asian summer rainfall. During decaying summers of El Niño with a weak EAWM$_{res}$ (Fig. 7c), East Asia is covered by largely positive geopotential height anomalies. These positive anomalies facilitate the WPSH to shift northward, causing substantial rainfall on the northwestern edge of this WPSH. In contrast, during decaying summers of the SEAWM$_{res}$–EN cases, the positive geopotential height anomaly over the WNP is confined to lower latitudes (Fig. 7f), which anchors the WPSH to the southward region. Thus, dry conditions are caused in northern China due to this southward location of the WPSH. In addition, the features of the 500-hPa geopotential height anomalies for La Niña are similar to those for El Niño (not shown).

5. Discussion: causes of the modulation effect of $EAWM_{res}$ on the ENSO–EASM relationship

The $EAWM_{res}$ tends to modulate the impact of the ENSO on the following EASM. One question relating to this is how does the $EAWM_{res}$ disrupt the ENSO–EASM relationship during the following summer when the winter monsoon has ended? Figure 8 presents the composite two-monthly averaged SST anomalies for the $WEAWM_{res}$–EN and $SEAWM_{res}$–EN groups. Comparing the SST anomalies between these two groups, one can see that the SST anomalies in the tropical region exhibit a similar spatial pattern, but the extra-tropical SST anomalies display a totally different distribution. This difference may arise from the effect of the $EAWM_{res}$. When El Niño is combined with a weak $EAWM_{res}$ (Fig. 8, left column), the extra-tropical SST anomalies are characterized by a tripole pattern with the warming signals in the North Pacific straddled by the cooling signals on its northern and southern sides. This pattern is significantly robust

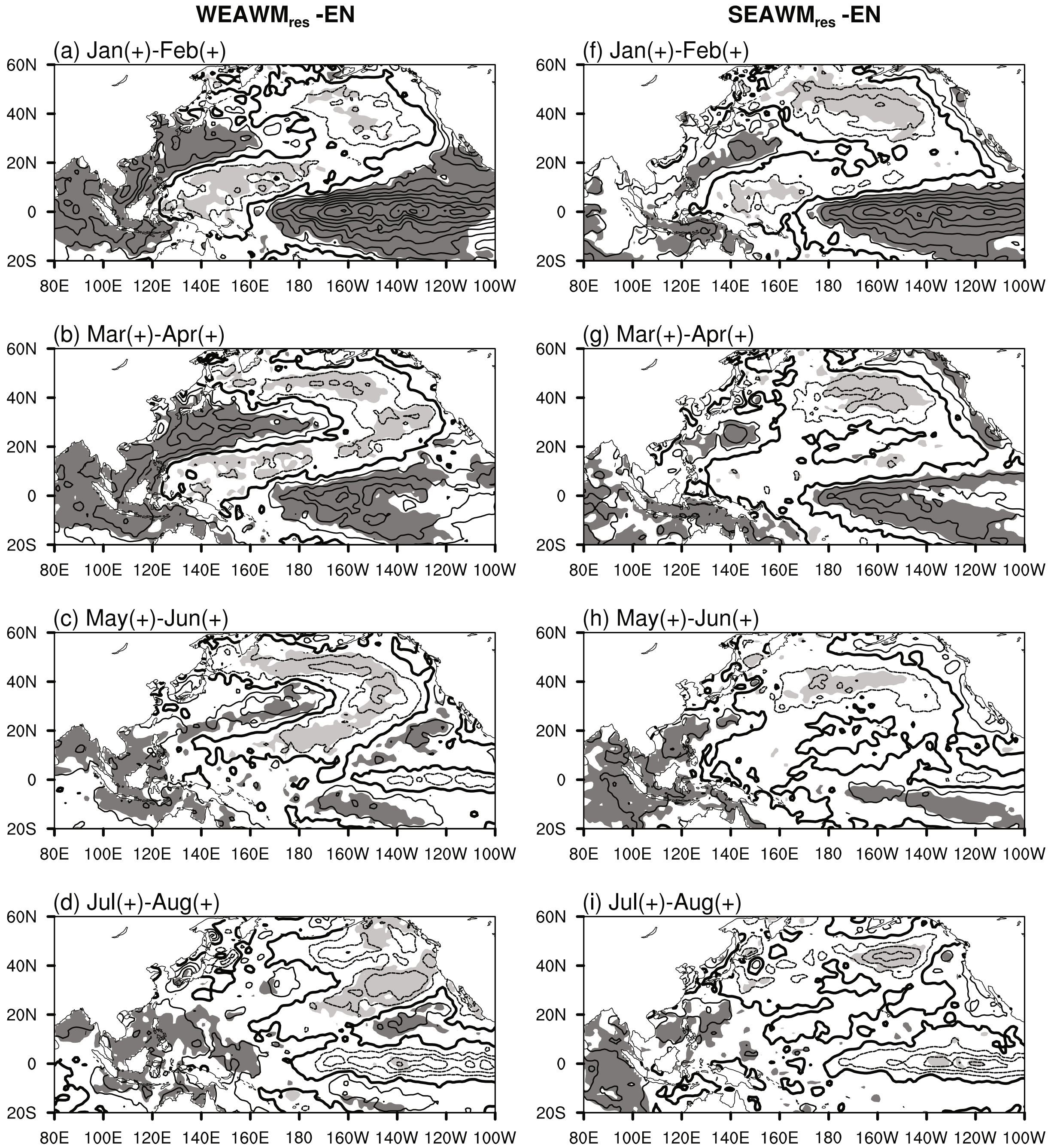

Fig. 8. Composite two-monthly average SST anomalies for the $WEAWM_{res}$–EN (left column) and $SEAWM_{res}$–EN (right column) groups. The contour interval is 0.2°C. The solid (dashed) lines denote positive (negative) anomalies. The shading indicates the 90% confidence level according to a two-tailed Student's *t*-test.

from winter to the following summer, although it is slightly weakened in late summer (Figs. 8a–d). In contrast, when El Niño is combined with a strong $EAWM_{res}$ (Fig. 8, right column), the North Pacific is mainly covered by negative SST anomalies persisting from winter to the following summer. Vimont et al. (2001) suggested that this extra-tropical tripole SST anomaly in the summer could generate negative vorticity anomalies over the western Pacific. This may favor the formation of the strong and large-scale WNP anticyclone during the $WEAWM_{res}$–EN cases, as shown in Fig. 4c and 7c. During the $SEAWM_{res}$–EN events, the negative SST anomalies in the North Pacific do not have this effect, thereby inducing a weak WNP anticyclone. The SST anomalies during the La Niña events have similar features to those for the El Niño events. Specifically, the extra-tropical SST anomaly presents a tripole pattern during the $SEAWM_{res}$–LN cases, with the negative SST anomaly in the North Pacific flanked by the positive SST anomaly on its northern and southern sides (not shown). According to the findings proposed by Vimont et al. (2001), this tripole SST anomaly pattern in the North Pacific favors a strengthening the WNP cyclone associated with La Niña during $SEAWM_{res}$–LN events. Therefore, the anomalous $EAWM_{res}$ tends to have an effect on the extra-tropical SST anomaly, which can persist into the next summer. Such extra-tropical SST anomalies may interfere with the influences of ENSO.

6. Summary

The modulation effect of the $EAWM_{res}$ on the ENSO–EASM relationship has been investigated based on observational data. ENSO events were divided into four groups according to $EAWM_{res}$ conditions: $WEAWM_{res}$–EN, $SEAWM_{res}$–EN, $WEAWM_{res}$–LN and $SEAWM_{res}$–LN. The composite results demonstrated that ENSO exerts a different influence on the following EASM under different $EAWM_{res}$ conditions. The anomalous summer rainfall differences occur most strikingly in northern China for El Niño events and in southwestern China for La Niña events. Northern China experiences excessive rainfall for the $WEAWM_{res}$–EN group, but deficient rainfall for the $SEAWM_{res}$–EN group. Meanwhile, southwestern China experiences less rainfall for the $WEAWM_{res}$–LN group and more rainfall for the $SEAWM_{res}$–LN group.

The low-level anomalous WNP anticyclone/cyclone is a key atmospheric system linking ENSO to the following summer's rainfall in East Asia. For the $WEAWM_{res}$-EN group, the weak $EAWM_{res}$ strengthens the anomalous WNP anticyclone associated with El Niño through inducing negative vorticity over the WNP. This strengthened WNP anticyclone occupies a large domain extending from the tropical western Pacific to mid-high latitudes, which can persist to the following summer. With the strong WNP anticyclone, the summertime WPSH tends to move northward and in turn favors abundant rainfall in northern China. In contrast, when El Niño happens together with a strong $EAWM_{res}$, the anomalous WNP anticyclone in winter is suppressed by the positive vorticity associated with a strong $EAWM_{res}$. This weakened WNP anticyclone is confined to the low latitudes and maintains from winter to the following summer, which anchors the WPSH to the southward region. With this southward location of the WPSH, less water vapor can be transported to the high latitudes, thereby leading to drought conditions in northern China. In the case of La Niña events, the anomalous WNP cyclone experiences a similar process under different $EAWM_{res}$ conditions. The WNP cyclone is enhanced during $SEAWM_{res}$–LN events and then causes a large amount of rainfall in southwestern China, whereas it is suppressed during $WEAWM_{res}$–LN events and results in drought conditions in southwestern China.

The $EAWM_{res}$ can modulate the wintertime atmospheric responses to ENSO. Thus, the question was raised as to how this modulation persists from winter to the following summer when the winter monsoon has ended. It was hypothesized that the features of the anomalous SST distribution may shed light on this question, and were thus examined. It was found that the anomalous $EAWM_{res}$ imparts its effect on the extra-tropical SST anomaly. An anomalous tripole SST pattern in the North Pacific can be observed from winter to the following summer during $WEAWM_{res}$–EN ($SEAWM_{res}$–LN) cases, which tends to generate anticyclonic (cyclonic) anomalies in the summer over the western Pacific. Therefore, the anomalous WNP anticyclone (cyclone) associated with El Niño (La Niña) is enhanced for $WEAWM_{res}$–EN ($SEAWM_{res}$–LN) cases. However, the extra-tropical tripole SST pattern does not occur during $SEAWM_{res}$–EN ($WEAWM_{res}$–LN) cases, being replaced by negative (positive) SST anomalies. Accordingly, the WNP anticyclone (cyclone) is much weaker in such cases.

Acknowledgements. This work was supported by the National Natural Science Foundation of China (Grant Nos. 41025017, 41230527 and 41205047).

REFERENCES

Chan, J. C. L., and W. Zhou, 2005: PDO, ENSO and the early summer monsoon rainfall over south China. *Geophys. Res. Lett.*, **32**, L08810, doi: 10.1029/2004GL022015.

Chang, C. P., Y. S. Zhang, and T. Li, 2000a: Interannual and interdecadal variations of the East Asian summer monsoon and tropical Pacific SSTs. Part I: Roles of the subtropical ridge. *J. Climate*, **13**, 4310–4325.

Chang, C. P., Y. S. Zhang, and T. Li, 2000b: Interannual and interdecadal variations of the East Asian summer monsoon and tropical Pacific SSTs. Part II: The meridional structure of the monsoon. *J. Climate*, **13**, 4326–4340.

Chen, W., 2002: Impacts of El Niño and La Niña on the cycle of the East Asian winter and summer monsoon. *Chinese J. Atmos. Sci.*, **26**, 595–610. (in Chinese)

Chen, W., H. F. Graf, and R. H. Huang, 2000: The interannual variability of East Asian winter monsoon and its relation to the summer monsoon. *Adv. Atmos. Sci.*, **17**, 48–60.

Chen, W., S. Yang, and R. H. Huang, 2005: Relationship between stationary planetary wave activity and the East Asian winter monsoon. *J. Geophys. Res.*, **110**, D14110, doi: 10.1029/2004JD005669.

Chen, W., J. Feng, and R. G. Wu, 2013: Roles of ENSO and PDO in the link of the East Asian winter monsoon to the following summer monsoon. *J. Climate*, **26**, 622–635.

Ding, R. Q., K.-J. Ha, and J. P. Li, 2010: Interdecadal shift in the relationship between the East Asian summer monsoon and the tropical Indian Ocean. *Climate Dyn*., **34**, 1059–1071.

Ding, Y. H., 1992: Summer monsoon rainfalls in China. *J. Meteor. Soc. Japan*, **70**, 373–396.

Ding, Y. H., 1994: *Monsoon over China*. Kluwer Academic Publishers, 420 pp.

Duchon, C. E., 1979: Lanczos filtering in one and two dimensions. *J. Appl. Meteor.*, **18**, 1016–1022.

Feng, J., W. Chen, C. Y. Tam, and W. Zhou, 2011: Different impacts of El Niño and El Niño Modoki on China rainfall in the decaying phases. *Int. J. Climatol.*, **31**, 2091–2101.

Huang, R. H., L. T. Zhou, and W. Chen, 2003: The progresses of recent studies on the variabilities of the East Asian monsoon and their causes. *Adv. Atmos. Sci.*, **20**, 55–69.

Huang, R. H., W. Chen, B. L. Yan, and R. H. Zhang, 2004: Recent advances in studies of the interaction between the East Asian winter and summer monsoons and ENSO cycle. *Adv. Atmos. Sci.*, **21**, 407–424.

Huang, R. H., and Y. F. Wu, 1989: The influence of ENSO on the summer climate change in China and its mechanism. *Adv. Atmos. Sci.*, **6**, 21–32.

Lau, K. M., 1992: East Asian summer monsoon rainfall variability and climate teleconnection. *J. Meteor. Soc. Japan*, **70**, 211–242.

Lau, K. M., and H. Y. Weng, 2001: Coherent modes of global SST and summer rainfall over China: An assessment of the regional impacts of the 1997–98 El Niño. *J. Climate*, **14**, 1294–1308.

Li, S. S., and S. W. Shou, 2000: Equatorial eastern Pacific SST and analysis on causes of summer floods/droughts in the Changjiang and Huaihe River basin. *Quarterly Journal of Applied Meteorology*, **11**, 331–338.

Lin, X. C., and S. Q. Yu, 1993: El Niño and rainfall during the flood season (June–August) in China. *Acta Meteorologica Sinica*, **51**, 434–441. (in Chinese)

Liu, Y. Q., and Y. H. Ding, 1992: Influence of El Niño on weather and climate in China. *Acta Meteorologica Sinica*, **6**, 117–131.

Rayner, N. A., D. E. Parker, E. B. Horton, C. K. Folland, L. V. Alexander, D. P. Rowell, E. C. Kent, and A. Kaplan, 2003: Global analyses of sea surface temperature, sea ice, and night marine air temperature since the late nineteenth century. *J. Geophys. Res.*, **108**, 4407, doi: 10.1029/2002JD002670.

Rong, X. Y., R. H. Zhang, and T. Li, 2010: Impacts of Atlantic sea surface temperature anomalies on Indo-East Asian summer monsoon-ENSO relationship. *Chinese Sci. Bull.*, **55**, 2458–2468.

Tao, S. Y., and L. X. Chen, 1987: A review of recent research on the East Asian summer monsoon in China. Monsoon Meteorology, C. P. Chang and T. N. Krishnamurti, Eds., Oxford University Press, 60–92.

Tomita, T., and T. Yasunari, 1996: Role of the northeast winter monsoon on the biennial oscillation of the ENSO/monsoon system. *J. Meteor. Soc. Japan*, **74**, 399–413.

Uppala, S. M., and Coauthors, 2005: The ERA-40 re-analysis. *Quart. J. Roy. Meteor. Soc.*, **131**, 2961–3012.

Vimont, D. J., D. S. Battisti, and A. C. Hirst, 2001: Footprinting: A seasonal connection between the tropics and mid-latitudes. *Geophys. Res. Lett.*, **28**, 3923–3926.

Wang, B., R. G. Wu, and X. H. Fu, 2000: Pacific-east Asian teleconnection: How does ENSO affect east Asian climate? *J. Climate*, **13**, 1517–1536.

Wang, H. J., 2002: The instability of the East Asian summer monsoon–ENSO relations. *Adv. Atmos. Sci.*, **19**, 1–11.

Wang, L., and W. Chen, 2010: Downward Arctic Oscillation signal associated with moderate weak stratospheric polar vortex and the cold December 2009. *Geophys. Res. Lett.*, **37**, L09707, doi: 10.1029/2010GL042659.

Wang, L., W. Chen, and R. H. Huang, 2008: Interdecadal modulation of PDO on the impact of ENSO on the east Asian winter monsoon. *Geophys. Res. Lett.*, **35**, L20702, doi: 10.1029/2008GL035287.

Weng, H. Y., K. Ashok, S. K. Behera, S. A. Rao, and T. Yamagata, 2007: Impacts of recent El Niño Modoki on dry/wet conditions in the Pacific rim during boreal summer. *Climate Dyn.*, **29**, 113–129.

Wu, R. G., and B. Wang, 2002: A contrast of the East Asian summer monsoon-ENSO relationship between 1962–77 and 1978–93. *J. Climate*, **15**, 3266–3279.

Wu, R. G., and B. P. Kirtman, 2007: Observed relationship of spring and summer East Asian rainfall with winter and spring Eurasian snow. *J. Climate*, **20**, 1285–1304.

Wu, R. G., S. Yang, Z. P. Wen, G. Huang, and K. M. Hu, 2012a: Interdecadal change in the relationship of southern China summer rainfall with tropical Indo-Pacific SST. *Theor. Appl. Climatol.*, **108**, 119–133.

Wu, R. G., Z.-Z. Hu, and B. P. Kirtman, 2003: Evolution of ENSO-related rainfall anomalies in East Asia. *J. Climate*, **16**, 3742–3758.

Wu, Z. W., J. P. Li, Z. H. Jiang, J. H. He, and X. Y. Zhu, 2012b: Possible effects of the North Atlantic Oscillation on the strengthening relationship between the East Asian summer monsoon and ENSO. *Int. J. Climatol.*, **32**, 794–800.

Xue, F., and C. Z. Liu, 2008: The influence of moderate ENSO on summer rainfall in eastern China and its comparison with strong ENSO. *Chinese Sci. Bull.*, **53**, 791–800.

Yang, S., K. M. Lau, and K. M. Kim, 2002: Variations of the East Asian jet stream and Asian-Pacific-American winter climate anomalies. *J. Climate*, **15**, 306–325.

Yoon, J., and S. W. Yeh, 2010: Influence of the Pacific Decadal Oscillation on the relationship between El Niño and the northeast Asian summer monsoon. *J. Climate*, **23**, 4525–4537.

Zhang, J. Y., L. Y. Wu, and W. J. Dong, 2011: Land-atmosphere coupling and summer climate variability over East Asia. *J. Geophys. Res.*, **116**(D5), doi: 10.1029/2010JD014714.

Zhang, R. H., A. Sumi, and M. Kimoto, 1996: Impact of El Niño on the East Asian monsoon: A diagnostic study of the '86/87 and '91/92 events. *J. Meteor. Soc. Japan*, **74**, 49–62.

Zhang, R. H., A. Sumi, and M. Kimoto, 1999: A diagnostic study of the impact of El Nino on the precipitation in China. *Adv. Atmos. Sci.*, **16**, 229–241.

Zhou, L.-T., and R. G. Wu, 2010: Respective impacts of the East Asian winter monsoon and ENSO on winter rainfall in China. *J. Geophys. Res.*, **115**, doi: 10.1029/2009JD012502.

Zhou, W., and J. C. L. Chan, 2007: ENSO and the South China Sea summer monsoon onset. *Int. J. Climatol.*, **27**, 157–167.

Zhou, W., C. Li, and J. Chan, 2006: The interdecadal variations of the summer monsoon rainfall over South China. *Meteor. Atmos. Phys.*, **93**, 165–175.